Carbonic Anhydrase XII Inhibitors Overcome P-Glycoprotein-Mediated Resistance to Temozolomide in Glioblastoma

Carbonic anhydrase XII inhibitors overcome P-glycoprotein-mediated resistance to temozolomide in glioblastoma

Iris C. Salaroglio[1,#], Prashant Mujumdar[2,#], Laura Annovazzi[3], Joanna Kopecka[1], Marta Mellai[3], Davide Schiffer[3], Sally-Ann Poulsen[2,*,#], Chiara Riganti[1,*,#]

[1]Department of Oncology, University of Torino, via Santena 5/bis, 10126 Torino, Italy

[2]Griffith Institute for Drug Discovery, Griffith University, Brisbane, Nathan, Queensland, 4111, Australia

[3]Neuro-Bio-Oncology Center, Fondazione Policlinico di Monza, via Pietro Micca 29, 13100, Vercelli, Italy

#Equal contributors

Running title

CAXII inhibitors reverse chemoresistance in glioblastoma

Keywords

carbonic anhydrase XII; P-glycoprotein; temozolomide; glioblastoma cancer stem cells

Financial support

Italian Association for Cancer Research (IG15232 to CR); Italian Ministry of University and Research (RBFR12SOQ1 and FABR2017 to C.R.); Australian Research Council (FT10100185 to S-A.P); Italian Institute for Security Service 2014-2017 (to ICS); Fondazione Umberto e Marilisa Caligara for Interdisciplinary Research 2018 (to ICS);

Fondazione Umberto Veronesi 2016 (to JK); Fondazione Policlinico di Monza (intramural grant to DS)

***Corresponding authors**: Prof. Sally-Ann Poulsen, Griffith Institute for Drug Discovery, Griffith University, Brisbane, Nathan, Queensland, 4111, Australia, phone: +61-7-37357825; email: s.poulsen@griffith.edu.au; Prof. Chiara Riganti, Department of Oncology, University of Torino; Via Santena 5/bis, 10126 Torino, Italy; phone: +39-011-6705857; fax: +39-011-6705845; email: chiara.riganti@unito.it

Conflict of interest disclosure

The authors declare no potential conflicts of interest.

Abstract word count: 169

***Total number of Table and Figure*:** 6

Total manuscript word count: 4512

Abstract

The role of carbonic anhydrase XII (CAXII) in the chemoresistance of glioblastoma is unexplored.

We found CAXII and P-glycoprotein co-expressed in neurospheres derived from 3/3 patients with different genetic backgrounds and low response to temozolomide (time to recurrence: 6-9 months). CAXII was necessary for the P-glycoprotein efflux of temozolomide and second-line chemotherapeutic drugs, determining chemoresistance in neurospheres.

Psammaplin C, a potent inhibitor of CAXII, re-sensitized primary neurospheres to temozolomide by reducing temozolomide efflux via P-glycoprotein. This effect was independent of other known temozolomide resistance factors present in the patients. The overall survival in orthotopic patient-derived xenografts of temozolomide-resistant neurospheres, co-dosed with Psammaplin C and temozolomide, was significantly increased over temozolomide-treated ($p<0.05$) and untreated animals ($p<0.02$), without detectable signs of systemic toxicity.

We propose that a CAXII inhibitor in combination with temozolomide may provide a new and effective approach to reverse chemoresistance in glioblastoma stem cells. This novel mechanism of action, via the interaction of CAXII and Pgp, ultimately blocks the efflux function of Pgp to improve glioblastoma patient outcomes.

Introduction

Glioblastoma (GB) is the most common and lethal adult primary brain tumor. The standard-of-care treatment comprises surgery, followed by radiotherapy and chemotherapy, then maintenance chemotherapy. Chemotherapy is based on the drug temozolomide (TMZ). With treatment, the increase in median survival rate for all patients is two months, while the median overall survival is 12-15 months (1). In the subset of GB patients with the O^6-methylguanine-DNA methyltransferase (MGMT) promoter methylated, the two year survival is higher at approximately 40% (1).

GB stem cells (SC), a subpopulation of GB that govern tumor initiation and recurrence, are particularly difficult to eradicate with chemotherapy (2). One cause is an elevated expression of P-glycoprotein (Pgp), an efflux pump that recognizes a broad spectrum of chemotherapeutics as substrates, including TMZ (3,4). The co-administration of a Pgp inhibitor with chemotherapy has met with limited success however, owing to serious side effects and toxicity (5). The identification of an alternative and safer mechanism to counter Pgp-mediated drug resistance in GB SC is of high unmet need.

Tumor acidosis is a hallmark of cancer (6). Membrane-bound carbonic anhydrases IX and/or XII (CA, EC 4.2.1.1) maintain the intracellular/extracellular pH for efficient Pgp activity (7), and optimal tumor growth, invasion and metastasis (6).

CAIX and CAXII specific inhibitors are increasingly being investigated as potential antitumor agents (8). Inhibitors of CAXII indirectly reduce Pgp activity and re-sensitize solid tumors to Pgp substrates with a magnitude similar to tariquidar, a validated Pgp inhibitor (9). CAXII and Pgp mRNA were detectable in GB patient (Tissue Cancer Genome Atlas, https://cancergenome.nih.gov), but CAXII (http://www.proteinatlas.org/ENSG00000074410-CA12/pathology) and Pgp (http://www.proteinatlas.org/ENSG00000085563-

ABCB1/pathology) proteins were poorly detectable by immunohistochemistry. This trend led us to hypothesize that CAXII and Pgp may be co-expressed in specific GB niches, e.g. SC-enriched niches, with CAXII maintaining optimum pH for Pgp activity.

CAXII is overexpressed in aggressive GB (10) and is a negative prognostic factor in infiltrating astrocytoma (11). CAXII is also highly expressed in 3D-culture of GB cells (neurospheres, NS) (12), a mimic of cancer-derived GB SC. The therapeutic implications surrounding CAXII have been poorly investigated in GB or GB SC. Here, we demonstrate that CAXII mediates resistance to TMZ in GB SC in a Pgp-dependent manner. We show that the combination of a CAXII inhibitor and TMZ substantially improve TMZ efficacy against GB SC in GB NS-patient-derived xeongrafts (GB-NS-PDX), and that this effect is independent of known factors of TMZ-resistance.

Methods

Reagents and plasticware. Plasticware for cell cultures was obtained from Falcon (Becton Dickinson, Franklin Lakes, NJ). Electrophoresis reagents were obtained from Bio-Rad Laboratories (Hercules, CA). The protein content of cell lysates was assessed using a BCA kit from Sigma Chemicals Co. (St. Louis, MO). Unless specified otherwise, all reagents were purchased from Sigma Chemicals Co.

Compounds synthesis and CAXII inhibition. Compounds were synthesized as in Supplementary Information (**Scheme 1**). CAXII activity was measured as detailed previously (13).

Cells. Primary human GB cells (CV17, 010627, No3) were obtained from surgical samples from Neurosurgical Units, Universities of Torino and Novara after written informed consent, and were used within passage 5. The samples were designated as patient#1, patient#2 and patient #3. Researchers performing the experiments were unaware of the genetic background or clinical outcome of the patients. The study was performed in accordance with the

Declaration of Helsinki and was approved by the Bio-Ethical Committee of University of Torino (#ORTO11WNST).The histological diagnosis of GB was performed according to WHO guidelines. *MGMT* methylation was detected by methylation-specific polymerase chain reaction and capillary electrophoresis (14). *EGFR* amplification, *IDH1/2* and *TP53* mutations, 1p/19q co-deletion were examined as described in (15). Cells were cultured as differentiated/adherent cells (AC) or NS as previously described (16), with minor modifications (17). For AC, DMEM supplemented with 1% v/v penicillin-streptomycin, 10% v/v fetal bovine serum (FBS; Lonza, Basel, Switzerland) was used. For NS, DMEM-F12 medium was supplemented with 1 M HEPES, 0.3 mg/ml glucose, 75 μg/ml $NaHCO_3$, 2 mg/ml heparin, 2 mg/ml bovine serum albumin, 2 mM progesterone, 20 ng/ml EGF, 10 ng/ml b-FGF. AC were obtained from dissociated NS cells, centrifuged at 1,200 × g for 5 min and seeded in AC medium. *In vitro* clonogenicity and self-renewal, and *in vivo* tumorigenicity were reported in (3). Cell phenotypic characterization is detailed in the Supplementary Materials. *Mycoplasma spp* contamination was assessed by PCR every 3 weeks; contaminated cells were discharged.

Immunoblotting. 20 μg protein extracts from whole cell lysate were subjected to SDS-PAGE and probed with the following antibodies: anti-CAXII (goat, #ab219641; Abcam, Cambridge, UK), anti-CAIX (rabbit, # ab15086; Abcam), anti-Pgp (mouse, clone C219; Millipore, Billerica, MA), anti-caspase 3 (mouse, clone C33, GeneTex, Hsinhu City, Taiwan). Plasma membrane-associated proteins were evaluated in biotinylation assays (7). Anti-β-tubulin (rabbit, # ab6046; Abcam) and anti-pancadherin (mouse, clone CH-19; Santa Cruz Biotechnology Inc., Santa Cruz, CA) antibody were used to confirm equal protein loading in whole cell and plasma-membrane associated extracts. In co-immunoprecipitation experiments, 100 μg of plasma membrane-associated proteins were immunoprecipitated with

anti-CAXII and anti-CAIX antibodies, using PureProteome protein A and protein G Magnetic Beads (Millipore).

Flow cytometry. Five×10^5 cells were re-suspended in culture medium containing 5% v/v FBS, incubated with anti-CAXII (Abcam) or anti-Pgp (mouse, clone MRK16; Kamiya, Seattle, WA) antibody, followed by the secondary Alexa488-conjugated antibody, fixed with 4% v/v paraformaldehyde and analyzed by the Guava® easyCyte flow cytometer, (InCyte software, Millipore). Control experiments included incubation of cells with non-immune isotypic antibody, followed by secondary antibody.

Proximity ligation assay (PLA). The CAXII-Pgp interaction was measured with the DuoLink In Situ kit (Sigma Chemicals Co), as per the manufacturer's instructions. The method employs mouse anti-human Pgp (mouse, clone UIC-2, Millipore) or rabbit anti-human CAXII (#102344; NovoPro, Shangai, China) antibodies. Cell nuclei were counterstained with 4',6-diamidino-2-phenylindole (DAPI). Cells were examined using a Leica DC100 fluorescence microscope (Leica Microsystem, Wetzlar, Germany). A minimum of five fields were examined for each experimental condition.

Confocal microscope analysis. 1×10^4 NS cells were seeded onto glass coverslips and collected by cyto-spinning. Cells were fixed using 4% paraformaldehyde for 15 minutes, washed with PBS and incubated for 1 h at room temperature with an anti-human CAXII (NovoPRo) or an anti-Pgp (Millipore) antibody. Samples were washed 5× with PBS and incubated for 1 h with tetramethylrhodamine isothiocyanate (TRITC)- or fluorescein isothiocyanate (FITC)-conjugated secondary antibodies (Sigma Chemicals Co.), respectively, then washed with PBS 4× and deionized water 1×. Cells were examined using a Leica TCS SP2 AOP confocal laser-scanning microscope. The number of yellow pixels, indicative of a Pgp-CAXII interaction, was calculated using the JACoP plug-in of the ImageJ software

(https://imagej.nih.gov/ij) and expressed as a percentage of the total green pixels (corresponding to Pgp) measured over a total of five fields per experiment.

Pgp ATPase activity. The assay was performed on Pgp-enriched membrane vesicles as detailed in (18). The rate of ATP hydrolysis, an index of Pgp catalytic cycle and a necessary step for substrate efflux, was measured. Results were expressed as nmol hydrolyzed phosphate (Pi)/min/mg proteins.

Doxorubicin and temozolomide accumulation. Doxorubicin content was measured fluorimetrically (7). The results were expressed as nmol doxorubicin/mg cell proteins. TMZ content was measured by liquid scintillation counting in cells incubated with 10 μM [^{3}H]-temozolomide (0.7 μCi/ml; Moravek Biochemical Inc., Brea, CA) for 24 h. The results were expressed as nmol [^{3}H]-temozolomide/mg cell proteins.

LDH release. The extracellular release of LDH, considered an index of cell damage, was measured as detailed previously (3). The extracellular LDH activity was calculated as a percentage of the total LDH activity in the dish.

Cell viability. Cell viability was evaluated using an ATPLite kit (PerkinElmer, Waltham, MA). The results were expressed as percentage of viable cells in each experimental condition versus untreated cells (considered 100% viable). To calculate the combination index (CI)**,** NS were incubated with TMZ and compound **1**, alone and then in combination, over the range of concentrations 10^{-10}- 10^{-3} M. CI values were calculated usingCalcuSyn software (www.biosoft.com/w/calcusyn.htm).

Generation of *Pgp*- and *CAXII*-knocked out (KO) clones. Five×10^{5} cells were transduced with 1 μg CRISPR pCas vectors (Origene, Rockville, MD) targeting *ABCB1/Pgp* or *CAXII* respectively, or with 1 μg non-targeting vector (Origene), following the manufacturer's instructions. Stable KO cells were selected from medium containing 1 μg/ml puromycin for 4 weeks.

***In Vitro* Plasma Stability.** Compound **1** was spiked into mouse plasma (Animal Resource Centre, Perth, Australia) to a concentration of 1000 ng/ml (DMSO/acetonitrile concentrations 0.2/0.4% v/v) at 37 °C for 4 h. At various time points, plasma samples were snap-frozen and analyzed by LC-MS (Micromass Xevo triple quadrupole mass spectrometer, Waters Co., Milford, MA) relative to calibration standards (**1** and diazepam as internal standard). The average concentration of test compound was expressed as a percentage of compound remaining relative to the sample quenched at 5 min.

***In Vitro* Metabolic Stability.** Metabolic stability was performed by incubating 1 μM compound **1** with 0.4 mg/ml mouse liver microsomes (Xenotech, Tokyo, Japan) at 37 °C, adding a NADPH-regenerating system, and subsequently quenching with acetonitrile (containing diazepam as internal standard) at 2, 30 and 60 min. A species scaling factor was used to convert the *in vitro* clearance (CL_{int}) to an *in vivo* CL_{int} (19). Hepatic blood clearance and hepatic extraction ratio (E_H) were calculated as described (20). E_H was used to classify compounds as low (< 0.3), intermediate (0.3–0.7), high (0.7–0.95) or very high (>0.95) extraction compounds.

***In Vitro* Cytochrome P450 (CYP) Stability.** Compound **1** (0.25 to 20 μM) was incubated with CYP substrate in human liver microsomes (batch #1410230; XenoTech LLC., Lenexa, KS, USA) at 37 °C. The total organic solvent concentration was 0.47% v/v. The reactions were initiated by adding a NADPH-regenerating system and quenched with ice cold acetonitrile containing analytical internal standard (0.15 μg/mL diazepam). Metabolite concentrations were determined by UPLC-MS (Waters/Micromass Xevo TQD triple-quadrupole) relative to calibration standards prepared in quenched microsomal matrix. The inhibitory effect of compound **1** was assessed based on the reduction in the formation of the specific CYP-mediated metabolite relative to a control for maximal CYP enzyme activity.

***In vivo* tumor growth.** In dose-dependent experimental sets 1×10^6 AC or NS cells, mixed with 100 µl Matrigel, were injected subcutaneously in female BALB/c *nu*/*nu* mice (weight: 19.6 g $\pm$ 2.4; Charles River Laboratories Italia, Calco). Animals were housed (5 per cage) under 12 h light/dark cycles in a barrier facility on HEPA-filtered racks and were fed with an autoclaved diet. Tumor dimensions were measured daily with calipers and growth calculated using the equation $(L \times W^2)/2$, where L = tumor length, W = tumor width. When the tumor reached a volume of 50 mm^3, animals were randomized (10 animals/group) and treated over 2 cycles of 5 consecutive days (days: 1-5; 11-15 after randomization) as detailed in **Supplementary Figure S6.** Animals were euthanized by injecting zolazepam (0.2 ml/kg) and xylazine (16 mg/kg) i.m. at day 30. Hemocromocytometric analyses were performed with a UniCel DxH 800 Coulter Cellular Analysis System (Beckman Coulter, Miami, FL) on 0.5 ml of blood collected immediately after euthanizing, using commercial kits from Beckman Coulter Inc.

In a second experimental set, 1×10^6 NS cells, stably transfected with the pGL4.51[luc2/CMV/Neo] vector encoding for luciferase (Promega Corporation), mixed with 150 µl sterile physiological solution, were stereotactically injected into the right caudatus nucleus into 6-8 week olds female BALB/c *nu*/*nu* mice (weight: 20.3 g $\pm$ 2.4), anesthetized with sodium phenobarbital (60 mg/kg) i.p. Tumor growth was monitored by *in vivo* bioluminescence (Xenogen IVIS Spectrum, PerkinElmer, Waltham, MA) at day 6, 14 and 24 post-implantation. At day 7, animals were randomized (6 animals/group) and treated with 2 cycles of 5 consecutive days (days: 7-11; 17-21 after randomization) as indicated in **Figure 5**. Animals were euthanized at day 30. Brains were fixed in 40 µg/ml paraformaldehyde at 4 °C overnight. Tumors were excised and the volume determined using calipers. Tumor sections were fixed overnight in 4% paraformaldehyde and stained with hematoxylin and eosin or immunostained for CAXII (Abcam), anti-Pgp (Millipore), Ki67 (mouse, clone KiS5;

Millipore), cleaved (Asp175)caspase 3 (rabbit, #9661; Cell Signaling Technology Inc., Danvers, MA), followed by a peroxidase-conjugated secondary antibody (Dako, Glostrup, Denmark). Stained sections were examined with a Leica DC100 microscope. In parallel, tumor tissue was homogenized for 30 s at 15 Hz, using a TissueLyser II device (Qiagen, Hilden, Germany) and clarified at 12000×g for 5 minutes. Protein (10 μg) from tumor lysates were used for the immunoblot analysis of Pgp, as reported above. In a third experimental set, animals with orthotopic tumors were monitored after the treatment detailed in **Figure 5**. Animals were euthanized when they showed signs of significantly compromised neurological function or loss of body weight >20%. Overall survival was defined as the time interval between tumor implant and euthanasia.

Animal care and experimental procedures were approved by the Bio-Ethical Committee of the Italian Ministry of Health (#122/2015-PR).

Statistical analysis. All data in the text and figures are provided as means ±SD. The results were analysed by a Student's t-test, using Statistical Package for Social Science (SPSS) software (IBM SPSS Statistics v.19). The Kaplan-Meier method was used to calculate overall survival of mice. Log rank test was used to compare the outcome of the treatment groups, using MedCalc® software (v.17.4). $p < 0.05$ was considered significant. Data analysis was performed blinded.

Results

Glioblastoma-derived neurospheres co-express CAXII and Pgp

The clinical, genomic and phenotypic data for the three GB patients of this study are provided in **Table 1** and **Supplementary Table S1**. The *MGMT* promoter status is partially methylated in patient #1, unmethylated in patient #2 and fully methylated in patient #3 (**Table 1)**. We generated primary cultures from patients #1-#3 and grew them as AC or NS.

NS had comparable levels of CAIX and CAXII protein, while only CAIX was detected in AC (**Figure 1a**). NS had higher levels of CAXII and Pgp on the cell surface than AC (**Figure 1b**). CAXII co-immunoprecipitated with Pgp (**Figure 1c**). The results of the PLA demonstrate that CAXII and Pgp are physically associated in the NS plasma-membrane (**Figure 1d**). Quantification of CAXII:Pgp co-localization, based on confocal laser-scanning microscopy, indicated that 58.67 ± 1.1 % of NS Pgp interacted with CAXII in the plasma-membrane of NS (**Figure 1e**).

The expression of Pgp and CAXII was independent of the different culture conditions between AC and NS (**Supplementary Figure S1**).

The addition of CAXII inhibitors to neurospheres reduces Pgp activity and increases retention and cytotoxicity of chemotherapeutic drugs

A compound panel comprising Psammaplin C (**1**), its derivatives (**2-4**) and the non-CAXII inhibitor control compound (**5**) (**Figure 2a)** was tested for the ability to indirectly reduce Pgp activity in NS. The more potent the CAXII inhibitor (lower K_i; **Supplementary Table S2**), the higher the reduction of Pgp activity (**Figure 2b**). The Pgp substrate doxorubicin accumulated to a greater extent (**Figure 2c**) and exhibited greater toxicity (**Figure 2d-e**) in AC than in NS. NS were refractory to doxorubicin. These characteristics were unchanged by compounds **1-5** in AC. In NS compounds **1** or **3**, the two most potent CAXII inhibitors, restored the intracellular doxorubicin concentration to a level comparable to AC (**Figure 2c**), partially restored the release of LDH induced by doxorubicin (**Figure 2d**) and reduced cell viability (**Figure 2e**).

Comparable effects were observed with the chemotherapeutic drugs etoposide, topotecan and irinotecan. These drugs are known substrates of Pgp (21) (**Supplementary Figure S2a-f**). As compound **1** was the most effective in restoring the effects of Pgp substrates in GB NS, it was selected for further characterization.

CAXII inhibition enhances temozolomide cytotoxicity in neurospheres by reducing Pgp activity

TMZ, a substrate and down-regulator of Pgp (4, 22), decreased Pgp expression in NS (**Figure 3a; Supplementary Figure S3a**). TMZ consistently reduced the amount of Pgp that co-immunoprecipitated with CAXII (**Figure 3b; Supplementary Figure S3b**) and the activity of Pgp (**Figure 3c**). Pgp expression (**Figure 3a; Supplementary Figure S3a**) and the interaction of Pgp and CAXII (**Figure 3b; Supplementary Figure S3b**) was unchanged by compound **1**, however Pgp-ATPase activity was reduced, even more so when in combination with TMZ (**Figure 3c**). Consequently, in NS compound **1** increased TMZ accumulation (**Figure 3d**), cell necrosis (**Figure 3e**), apoptosis (**Figure 3f**) and reduced viability in the presence of TMZ (**Figure 3g**), to the extent observed in *Pgp*-KO NS clones (wherein the levels of CAXII were unaltered) or in AC (**Figure 3d-g; Supplementary Figure S3c-d).** In *Pgp*-KO NS clones compound **1** did not enhance the effect of TMZ on reduced cell viability (**Figure 3g**), suggesting that Pgp is the ultimate – although indirect – target of compound **1**. The isobologram analysis in NS (**Supplementary Figure S4a-c**) indicated a CI of TMZ and compound **1** equal to 0.08838 for patient #1, 0.07017 for patient #2 and 0.1775 for patient #3. *CAXII*-KO NS clones had the same levels of Pgp in whole cell (**Figure 4a; Supplementary Figure S5a**) and plasma-membrane extracts (**Figure 4b; Supplementary Figure S5b**) than in NS or NS treated with a non-targeting vector. Similarly, the amount of plasma-membrane-associated Pgp in NS did not change when NS were treated with 10 nM of compound **1** (**Figure 4b; Supplementary Figure S5b)**. However, when plasma-membrane extracts of *CAXII*-KO NS clones were immuno-precipitated with an anti-CAXII antibody, Pgp was undetectable in the immunoprecipitated extracts (**Figure 4c; Supplementary Figure S5c**), confirming a strong and specific interaction between the two proteins. *CAXII*-KO NS clones had lower Pgp-ATPase activity than wild-type NS (**Figure 4d**) even when the levels of Pgp

were the same. TMZ further reduced Pgp-ATPase activity in *CAXII*-KO NS clones (**Figure 4d**) and produced the same phenotypic response as in AC, namely TMZ accumulation (**Figure 4e**) and cytotoxicity (**Figures 4f-h; Supplementary Figure S5d**).

CAXII inhibition restores the efficacy of temozolomide in tumors derived from resistant glioblastoma neurospheres *in vivo*

Compound **1** was stable in Balb/c mice plasma (half-life >240 min) (**Supplementary Table S3**) and showed low potential to inhibit major drug metabolizing CYP P450 enzymes (**Supplementary Table S4**).

Following identification of the dosing schedule that maximally reduced the tumor growth of AC *in vivo* (**Supplementary Figure S6a**) with significantly less effect against NS (**Supplementary Figure S6b-c**), we co-administered compound **1** in mice bearing patient #2-derived NS at two dosages, 38 ng/kg and 3800 ng/kg, the former according to the CAXII K_i; the latter to limit hematic/lymphatic clearance. Compound **1** did not reduce AC- or NS-derived tumor growth. When compound **1** was combined with TMZ, TMZ efficacy in AC-derived tumors was unchanged; however in NS-derived tumors TMZ efficacy was enhanced in a dose-dependent manner (**Supplementary Figure S6b-c**). Moreover, the combined treatment did not elevate hematopoiesis, liver, kidney or muscle toxicity compared to TMZ-only treatment (**Supplementary Table S5**). Consistent with the *in vitro* setting (**Figure 3f**), the growth of *Pgp*-KO NS-derived tumors was reduced by TMZ, while the growth of scrambled-transduced tumors was not (**Supplementary Figure S6d**). Compound **1**, at the dosage of 3800 ng/kg, enhanced the anti-tumor effect of TMZ in animals bearing scrambled-NS but not in animals bearing *Pgp*-KO NS (**Supplementary Figure S6d**) that lack this indirect target of compound **1**.

In orthotopic GB-NS-PDX neither compound **1** nor TMZ alone reduced tumor growth, with the exception of tumors derived from patient #3, wherein the genetic profile and clinical

history were suggestive of a more favorable response to TMZ (**Table 1**). The combination of compound **1** and TMZ significantly decreased tumor growth in all three GB-NS-PDX (**Figure 5a-b**) and increased overall survival (**Figure 5c)**. Although TMZ reduced the expression of Pgp in CAXII-positive tumors (**Figure 5d-f**), it did not reduce intratumor proliferation or increase apoptosis (**Figure 5d-e**).Compound **1** did not changed these parameters. The combined use of compound **1** and TMZ reduced Pgp expression in tumors (**Figure 5d-f)** as it did in NS cultured *in vitro* (**Figure 3a**). The combination also rescued the anti-proliferative and pro-apoptotic effects of TMZ, as demonstrated by the reduced intratumor positive staining for Ki67 and by the increased activation of caspase 3 (**Figure 5d-e**).

Discussion

We analyzed samples from three GB patients that experienced a variable but poor clinical response to TMZ. The patients had different genetic backgrounds however the NS-derived from all patients co-expressed CAXII and Pgp, suggesting a relationship that may represent an ancestral feature of GB SC, independent of genetic alterations or environmental conditions (such as different culture conditions). Notably, up to 60% of the Pgp in the plasma-membrane of NS was found to interact with CAXII. This indicates that the enzymatic activity of CAXII may act to influence the microenvironment pH for the co-localized Pgp. We are currently investigating the mechanisms of up-regulation of Pgp and CAXII expression in NS and the nature of interaction between these two proteins. To the best of our knowledge, ours is the first work showing an increased CAXII expression in GB NS derived from primary tumors. Until now, there have been no reports on the role of CAXII in the response to chemotherapy in NS. Based on our previous observations in Pgp-expressing solid cancer cell lines (7,9), we hypothesized that CAXII inhibitors may reverse the Pgp-mediated drug-resistance in GB NS, wherein Pgp activity is enhanced by CAXII activity. Even though CAIX is expressed in NS

and is important in GB pathogenesis (23), our data indicate no significant role for CAIX in the chemoresistance of NS.

We recently synthesized Psammaplin C (compound **1** in this manuscript), one of the most potent CAXII inhibitors ever reported (24). We synthesized a panel of related sulfonamides (**2-4**) and the control compound **5**, which is identical to **1** but lacks the sulfonamide moiety. This panel enabled the structure-activity relationships (SAR) between CAXII inhibition and indirect Pgp inhibition to be established. The strongest inhibitor of CAXII, compound **1**, was the most effective in rescuing the cytotoxicity of all tested Pgp substrates: topoisomerase I/II inhibitors topotecan, irinotecan, etoposide and doxorubicin. These drugs are under evaluation in clinical trials as second-line treatments for GB and in GB patients that are refractory to TMZ (25). Our findings suggest CAXII inhibitors may substantially enhance the efficacy of these agents, being particularly effective against GB NS, where improvement of current therapy is desperately sought.

Most importantly, compound **1** rescued the efficacy of TMZ, the first-line drug in GB treatment. TMZ fails to eradicate GB SC, owing to a combination of *MGMT* status, cell survival/anti-apoptotic pathways driven by *EGFR* amplification, mutations in IDH1/2 and *TP53*, hypoxia, niches rich of growth factors (2). The three patient-derived NS analyzed in this work had slight variation in their *in vitro* and *in vivo* sensitivity and clinical response to TMZ, likely as a consequence of their different genetic background. In general, however, NS from all patient samples were more resistant to TMZ than corresponding AC. The co-administration of compound **1** rescued sensitivity to TMZ, independent of *MGMT* status or other genetic alterations, suggesting that inhibition of CAXII may overcome Pgp-mediated resistance to TMZ.

Our findings in *Pgp*-KO and *CAXII*-KO NS support the hypotheses that i) in addition to the *MGMT* methylation status and other known genetic alterations determining resistance to

TMZ, the presence of Pgp plays a pivotal role in NS resistance to chemotherapy; ii) CAXII inhibition overcomes this resistance by reducing Pgp activity. It is probable that the interaction of CAXII with Pgp sustains the activity of Pgp, and that interfering with CAXII by treatment with either compound **1** or genetic knockout significantly reduces ATPase activity. Notably, this genetic or pharmacological inhibition did not alter the amount of surface Pgp. As Pgp mediates TMZ efflux (4), targeting CAXII increases the intracellular retention of TMZ to restore its cytotoxic effects.

The strong synergism observed with TMZ and compound **1** further enforces the hypothesis that they are involved in the same pathway leading to inhibition of Pgp efflux activity. The ability of compound **1** to reduce Pgp activity together with its potency and selectivity for CAXII over other CAs, contribute to making compound **1** highly effective against GB NS. Furthermore, CAXII has minimal expression in healthy cells (https://www.proteinatlas.org/ENSG00000074410-CA12/tissue). This is a major advantage as targeting CAXII to indirectly reduce Pgp activity provides a selective GB SC-targeting tool and avoids the *in vivo* toxicity associated with using direct Pgp inhibitors (5). Furthermore, the *in vitro* results obtained from treatment of GB-SC with a combination of compound **1** and second-line chemotherapeutic drugs (all substrates of Pgp) may open the way for new combination therapies with the potential to lower the chemotherapy dose required to achieve significant GB reduction.

In line with the TMZ resistance observed in NS cultures and the clinical response of the corresponding patient to TMZ, two of the three GB-NS-PDX were refractory to TMZ. The third xenograft - generated from the patient with the most favorable genetic profile toward TMZ sensitivity, longest time to recurrence after TMZ treatment and longest overall survival - was partially sensitive to TMZ. In accordance with the *in vitro* findings tumor growth in compound **1** only treated GB-NS-PDX was not reduced, however compound **1** in

combination with TMZ significantly improved the anti-tumor activity over the TMZ-only cohort and increased the overall survival, likely as a consequence of the co-expression of CAXII and Pgp in these NS-derived tumors. Furthermore, the combination of TMZ and compound **1** reduced the intratumor level of Pgp, and recapitulated the same cytotoxic events observed in NS cultures.

Recently the combination of the CAIX/CAXII inhibitor SLC-0111 (100 mg/kg, daily over 14 days) with TMZ (100 mg/kg once every 7 days over 14 days) reduced GB growth compared to TMZ only. The authors speculate that the mechanism of SLC-0111 may be mediated by CAIX together with increased DNA damage (26). This study did not however have the benefit of the inactive probe/active compound combination (compound **5** and **1** in our study) to contribute evidence to support the hypothesis that CAIX was the predominant target of SLC-0111. Our work may provide an additional explanation for the effect of SLC-0111, correlating its efficacy with CAXII inhibition causing indirect inhibition of Pgp and increased intratumor retention of TMZ. Of note, compound **1** was effective at a substantially lower dosage than SLC-0111. Additionally, compound **1** was devoid of toxicity and did not exacerbate TMZ side-effects, suggesting an appropriate efficacy and safety window with this combination treatment.

In summary, we have investigated for the first time the expression and therapeutic implication of CAXII in the highly chemorefractory GB SC-component of GB. We propose that CAXII and Pgp co-expression is a new hallmark of chemoresistance in GB NS. This relationship represents a previously unknown mechanism of TMZ resistance in GB-derived NS, wherein CAXII contributes to the Pgp-mediated resistance to TMZ and topoisomerase I/II inhibitors in patient-derived GB NS. The detection of CAXII in primary GB samples by routine immunohistochemistry techniques may be difficult however as CAXII is restricted to the SC-component that represents only a small portion of tumor bulk. This restricted

distribution may limit the potential use of CAXII as a predictive marker of low TMZ-response. CAXII may however represent an exciting new therapeutic target in GB patients resistant to TMZ and with a significant component of SC identified by pathology analysis. Pharmacological inhibition of CAXII rescues the efficacy of TMZ, independently of genetic alterations commonly associated with TMZ-resistance. Our results may form a basis to warrant clinical validation of a new combinatorial therapy, based on a CAXII-inhibitor with TMZ and/or topoisomerase I/II inhibitor, as more effective treatments to eliminate GB SC compared to current treatment options.

Authors contributions

ICS and LA performed in vitro and in vivo biological assays; PM synthesized the compounds; MM performed the histopathological and genetic characterization of the primary samples; JK analyzed the data of in vitro and in vivo biological assays; DS analyzed histopathological and genetic characterization, and collected the data of the patient clinical follow-up; S-AP and CR conceived the study, supervised the work and wrote the manuscript.

Acknowledgments

We are grateful to Professor Supuran for CA enzyme inhibition assays, to Mr. Costanzo Costamagna, Department of Oncology, University of Torino, for technical assistance.

References

1. Stupp R, Taillibert S, Kanner A, Read W, Steinberg DM, Lhermitte B, *et al*. Effect of Tumor-Treating Fields Plus Maintenance Temozolomide vs Maintenance Temozolomide Alone on Survival in Patients With Glioblastoma: A Randomized Clinical Trial. *JAMA* **2017**;318:2306–16

2. Auffinger B, Spencer D, Pytel P, Ahmed AU, Lesniak MS. The role of glioma stem cells in chemotherapy resistance and glioblastoma multiforme recurrence. *Expert Rev. Neurother* **2015**;15:741–52

3. Riganti C, Salaroglio IC, Caldera V, Campia I, Kopecka J, Mellai M, *et al*. Temozolomide downregulates P-glycoprotein expression in glioblastoma stem cells by interfering with the Wnt3a/glycogen synthase-3 kinase/β-catenin pathway. *Neuro Oncol* **2013**;15:1502–17

4. Munoz JL, Wlaker ND, Scotto KW, Rameshwar P. Temozolomide competes for P-glycoprotein and contributes to chemoresistance in glioblastoma cells. *Cancer Lett* **2015**;367:69–75

5. Callaghan R, Luk F, Bebawy M. Inhibition of the multidrug resistance P-glycoprotein: time for a change of strategy? *Drug Metab. Dispos* **2014**;42**:**623–31

6. Corbet C, Feron O. Tumour acidosis: from the passenger to the driver's seat. *Nat Rev Oncol* **2017***;*17:577–93

7. Kopecka J, Campia I, Jacobs A, Frei AP, Ghigo D, Wollscheid B, *et al.* Carbonic anhydrase XII is a new therapeutic target to overcome chemoresistance in cancer cells. *Oncotarget* **2015**;6:6776–93

8. Gondi G, Mysliwietz J, Hulikova A, Jen JP, Swietach P, Kremmer E, *et al.* Antitumor efficacy of a monoclonal antibody that inhibits the activity of cancer-associated carbonic anhydrase XII. *Cancer Res* **2013**;73:6494–503

9. Kopecka J, Rankin GM, Salaroglio IC, Poulsen SA, Riganti C. P-glycoprotein-mediated chemoresistance is reversed by carbonic anhydrase XII inhibitors. *Oncotarget* **2016**;7:85861–75

10. Beckner ME, Pollack IF, Nordberg ML, Hamilton RL. Glioblastomas with copy number gains in EGFR and RNF139 show increased expressions of carbonic anhydrase genes transformed by ENO1. *Biochim Biophys Acta Clin* **2016**;5:1–15

11. Haapasalo J, Hilvo M, Nordfors K, Haapasalo H, Parkkila S, Hyrskyluoto A, *et al*. Identification of an alternatively spliced isoform of carbonic anhydrase XII in diffusely infiltrating astrocytic gliomas. *Neuro Oncol*. **2008**;10:131–38

12. Battke C, Kremmer E, Mysliwietz J, Gondi G, Dumitru C, Brandau S, *et al*. Generation and characterization of the first inhibitory antibody targeting tumour-associated carbonic anhydrase XII. *Cancer Immunol Immunother* **2011**;60:649–58.

13. Morris JC, Chiche J, Grellier C, Lopez M, Bornaghi LF, Maresca A, *et al*. Targeting hypoxic tumor cell viability with carbohydrate-based carbonic anhydrase IX and XII inhibitors. *J Med Chem* **2011**;54:6905–18

14. Mellai M, Caldera V, Annovazzi L, Chiò A, Lanotte M, Cassoni P, *et al.* MGMT promoter hypermethylation in a series of 104 glioblastomas. *Cancer Genomics Proteomics* **2009**;6:219–27

15. Mellai M, Piazzi A, Caldera V, Monzeglio O, Cassoni P, Valente G, *et al.* IDH1 and IDH2 mutations, immunohistochemistry and associations in a series of brain tumors. *J Neurooncol* 2011;**105:**345–57

16. Reynolds BA, Tetzlaff W, Weiss S. A multipotent EGF-responsive striatal embryonic progenitor cell produces neurons and astrocytes. *J Neurosci* **1992**;12:4565–74

17. Caldera V, Mellai M, Annovazzi L, Piazzi A, Lanotte M, Cassoni P, *et al.* Antigenic and Genotypic Similarity between Primary Glioblastomas and Their Derived Neurospheres. *J Oncol* **2011;**2011:e314962

18. Kopecka J, Salzano G, Campia I, Lusa S, Ghigo D, De Rosa G, *et al*. Insights in the chemical components of liposomes responsible for P-glycoprotein inhibition. *Nanomedicine* **2014**;10:77**–**87

19. Ring BJ, Chien JY, Adkison KK, Jones HM, Rowland M, Jones RD, *et al*. PhRMA CPCDC initiative on predictive models of human pharmacokinetics, part 3: comparative assessement of prediction methods of human clearance. *J Pharm Sci* **2011***;*100:4090−110

20. Obach RS. Prediction of human clearance of twenty-nine drugs from hepatic microsomal intrinsic clearance data: An examination of in vitro half-life approach and nonspecific binding to microsomes. *Drug Metab. Dispos* **1999**;27:1350−59

21. Gottesman MM, Fojo T, Bates SE. Multidrug resistance in cancer: role of ATP-dependent transporters. *Nat Rev Cancer* **2002**;2:48–58

22. Zhang R, Saito R, Shibahara I, Sugiyama S, Kanamori M, Sonoda Y, *et al*. Temozolomide reverses doxorubicin resistance by inhibiting P-glycoprotein in malignant glioma cells. *J Neurooncol* **2016**;126:235–42

23. Proescholdt MA, Merrill MJ, Stoerr EM, Lohmeier A, Pohl F, Brawanski A. Function of carbonic anhydrase IX in glioblastoma multiforme. *Neuro On*col **2012**;14:1357–66

24. Mujumdar P, Teruya K, Tonissen KF, Vullo D, Supuran CT, Peat TS, *et al*. An unusual natural product primary sulfonamide: synthesis, carbonic anhydrase inhibition, and protein X-ray structures of Psammaplin C. *J Med Chem **2016**;*59:5462–70

25. Carvalho BF, Fernandes AC, Almeida DS, Sampaio LV, Costa A, Caeiro C, *et al.* Second-line chemotherapy in recurrent glioblastoma: a 2-cohort study. *Oncol Res Treat **2015***; 38:348–54

26. Boyd NH, Walker K, Fried J, Hackney JR, McDonald PC, Benavides GA, *et al*. Addition of carbonic anhydrase 9 inhibitor SLC-0111 to temozolomide treatment delays glioblastoma growth in vivo. *JCI. Insight* **2017**;2**:**pii: 92928

Table 1. Patient clinical, pathological and genetic data

	Patient #1	Patient #2	Patient #3
Age at diagnosis	57	53	61
Sex	M	F	M
Histological grade	IV	IV	IV
Therapy	Surgery + radiotherapy + chemotherapy	Surgery + radiotherapy + chemotherapy	Surgery + radiotherapy + chemotherapy
Time to recurrence (months)	7	6	9
Post-recurrence therapy	Re-resection + radiotherapy	Radiotherapy	Radiotherapy+ chemotherapy
Overall survival (months)	12	9	18
MGMT status	Partially methylated	Fully unmethylated	Fully methylated
EGFR status	Not amplified	Not amplified	Amplified
IDH1 status	Mutated (395G>A)	Mutated (395G>A)	Wild-type
IDH2 status	Wild-type	Wild-type	Wild-type
TP53	Wild-type	Mutated (380C>T)	Wild-type
1p/19q co-deletion	Present	Absent	Absent

Anagraphical, pathological, clinical and genetic data of patients of samples were used in the study. Radiotherapy: 60 Gy (30 fractions). Chemotherapy: 75 mg/m^2 temozolomide (TMZ), *per os*, daily, concurrently to radiotherapy, followed by 200 mg/m^2 TMZ, *per os*, days 1-5, every 28 days, 6 cycles. Post-recurrence therapy: radiotherapy: 60 Gy (30 fractions); chemotherapy: 80 mg/m^2 carmustine (BCNU), days 1-3, every 8 weeks, 3 cycles. Time to recurrence: time between the surgery and the appearance of tumor relapse at magnetic resonance imaging (MRI). Overall survival: time between diagnosis and patient death. MGMT: O^6-methylguanine-DNA methyltransferase. Fully methylated: promoter methylation of both alleles; partially methylated: promoter methylation of one allele. EGFR: epithelial

growth factor receptor. Amplified: > 2 copies of EGFR genes; not amplified: < 2 copies of EGFR gene. IDH: isocitrate dehydrogenase.

Figures legends

Figure 1. CAXII and Pgp are co-expressed and associated in glioblastoma-derived neurospheres

Primary GB cells derived from three patients (#1, #2, #3) were cultured as adherent cells (AC) or as neurospheres (NS). **a.** Cells were lysed and immunoblotted with the indicated antibodies. The figure is representative of one out of three experiments. **b.** Cell surface expression of CAXII and Pgp was detected by flow cytometry in replicate. The histograms are representative of one out of three experiments. **c.** Plasma-membrane extracts were immuno-precipitated (IP) with anti-CAXII or anti-CAIX antibodies, then immunoblotted (IB) with an anti-Pgp antibody. In a complementary experimental set, plasma-membrane extracts were immuno-precipitated with an anti-Pgp antibody and immunoblotted with an anti-CAXII antibody, to confirm the specificity of the interaction between Pgp and CAXII. no Ab: #2 NS sample immunoprecipitated without antibody. An aliquot of the extracts before the immunoprecipitation was loaded and probed with an anti-pancadherin antibody, as control of equal protein loading. The figure is representative of one out of three experiments. **d.** Proximity ligation assay between CAXII and Pgp in patient #2 AC and NS. Bl: cells incubated without primary antibodies; Ab: cells incubated with primary antibodies. Blue: nuclear staining (DAPI); green: Pgp/CAXII interaction. The image is representative of one out of three experiments. A minimum of five fields/experiment were examined. Bar: 10 μm (10× ocular lens; 63× objective lens). **e**. Immunofluorescence detection of plasma-membrane associated CAXII and Pgp in non-permeabilized NS from patient #2, by confocal microscope analysis. The image is representative of one out of three experiments. A minimum of five fields/experiment were examined. Bar: 10 μm (10× ocular lens; 60× objective lens).

Figure 2. CAXII inhibition reduces Pgp activity and increases cytotoxicity of doxorubicin in glioblastoma-derived neurospheres

a. Chemical structures of CAXII inhibitors used. For panels **b-d**: pooled data of patients #1, #2 and #3 are presented as means±SD (n=3 independent experiments for each patient). Violet, orange and blue circles represent the mean of technical replicates of patients #1, #2 and #3. **b.** Spectrophotometric measure of Pgp ATPase activity, detected in triplicates in NS, grown for 24 h in fresh medium (-) or in medium containing 10 nM compounds **1-5**. *p<0.02: compound **4** vs. untreated (-) cells: ***p<0.001: compounds **1** and **3** vs. untreated (-) cells (Student's t-test). **c.** Fluorimetric detection of doxorubicin (dox) accumulation, measured in duplicates in cells treated 24 h with 5 μM dox, alone (-) or in the presence of 10 nM compounds **1-5**. *p<0.05: NS treated with compound **4** vs. corresponding AC ***p<0.001: untreated NS or treated with compounds **2** and **5** vs. corresponding AC; $^{\#\#}$p<0.002: NS treated with compound **1** and **3** vs. untreated (-) NS (Student's t-test). **d.** Release of LDH, measured spectrophotometrically in duplicates, in cells grown for 24 h in fresh medium (-) or in media containing 10 nM compounds **1-5**, in the absence or presence of 5 μM dox. *p<0.05: treated AC/NS vs. corresponding "- dox" cells; ***p<0.001: treated AC/NS vs. corresponding "- dox" cells; $^{\#\#}$p<0.002: NS treated with compound **1** and **3** vs. "+dox" NS (Student's t-test). **e.** Viability of cells, measured by a chemiluminescence-based assay in quadruplicates, after 72 h in fresh medium (-) or in media containing 10 nM compounds **1-5**, in the absence or presence of 5 μM dox. ***p<0.001: treated AC/NS vs. corresponding "- dox" cells; $^{\#\#\#}$p<0.001: NS treated with compound **1, 3** and **4** vs. "+dox" NS (Student's t-test).

Figure 3. CAXII pharmacological inhibition restores temozolomide cytotoxicity in glioblastoma-derived neurospheres

NS were grown for 48 h (panels **a**-**f**) or 72 h (panel **g**) in fresh medium (-) or in medium containing 50 μM temozolomide (T) or 10 nM compound **1**, alone or in association. Panels **b, c, d, f**: pooled data of patients #1, #2 and #3 are presented as means±SD (n=4 independent

experiments for each patient). Violet, orange and blue circles represent the mean of technical replicates of #1, #2 and #3. AC were included as control of cells with undetectable CAXII levels. **a.** Patient #2 NS were lysed and immunoblotted for Pgp and CAXII. The figure is representative of one out of three experiments. **b.** Plasma-membrane extracts were immunoprecipitated (IP) with an anti-CAXII antibody, then immunoblotted (IB) with an anti-Pgp antibody. no Ab: sample immuno-precipitated without antibody. An aliquot of the extracts before the immunoprecipitation was loaded and probed with an anti-pancadherin antibody, as control of equal protein loading. The figure is representative of one out of three experiments. **c.** Spectrophotometric measure of Pgp ATPase, detected in triplicates in NS. *p<0.01: T-treated vs. untreated (-) cells;** p<0.01: **1**-treated vs. untreated (-) cells; ***p<0.001: T+**1**-treated vs. untreated (-) cells; $^{\#}$p<0.05: T+**1**-treated vs. T-treated cells (Student's t-test). **d.** Intracellular content of temozolomide (TMZ), measured in duplicates after cell radiolabelling. NS clones knocked out for Pgp (KO#1, KO#2) and AC were included as control of cells with undetectable expression of Pgp. ***p<0.001: all experimental conditions vs. untreated (-) NS (Student's t-test). **e.** LDH release, measured spectrophotometrically in duplicates. ***p<0.001: all experimental conditions vs. untreated (-) AC/NS; $^{\#\#\#}$p<0.001: T+**1**-treated, T+KO1/KO2 cells vs. T-treated cells; §§§p<0.001: T+KO1/KO2 cells vs. KO1/KO2 cells (Student's t-test). **f.** Patient #2 NS, incubated as reported in **a** and/or knocked out for Pgp, were lysed and immunoblotted for procaspase and cleaved caspase 3. The figure is representative of one out of three experiments. **g.** Cell viability measured by a chemiluminescence-based assay in quadruplicates. ***p<0.001: all experimental conditions vs. untreated (-) AC/NS; $^{\#\#}$p<0.005: T+**1**-treated vs. T-treated cells; $^{\#\#\#}$p<0.001: T+KO1/KO2 or T+**1**+ KO1/KO2 cells vs. T-treated cells; §§§p<0.001: T+KO1/KO2 or T+**1**+ KO1/KO2 cells vs. KO1/KO2 cells (Student's t-test).

Figure 4. CAXII knocking-out restores sensitivity to temozolomide in glioblastoma-derived neurospheres

NS were grown for 48 h (panels **a**-**g**) or 72 h (panel **h**) in fresh medium (-) or in medium containing 50 μM temozolomide (T) or 10 nM compound **1**, alone or in association. Panels **d, e, f, h**: pooled data of patients #1, #2 and #3 are presented as means±SD (n=4 independent experiments for each patient). Violet, orange and blue circles represent the mean of technical replicates of #1, #2 and #3. AC were included as control of cells with undetectable CAXII levels. **a.** Patient #2 NS were growth in fresh medium (-), transduced with a non-targeting vector (scrambled vector; scr) or with two CRISPR pCas *CAXII*-targeting vectors (KO#1, KO#2), lysed and immunoblotted with the indicated antibodies. The figure is representative of one out of three experiments. **b**. Plasma-membrane extracts were probed with an anti-Pgp antibody, or an anti-pancadherin antibody, as control of equal protein loading. The figure is representative of one out of three experiments. **c**. Plasma-membrane extracts from patient #2 *CAXII*-KO NS clones were immunoprecipitated (IP) with an anti-CAXII antibody and immunoblotted (IP) with an anti-Pgp antibody. no Ab: sample immuno-precipitated without antibody. An aliquot of the extract before the immunoprecipitation was loaded and probed with an anti-pancadherin antibody, as control of equal protein loading. The figure is representative of one out of three experiments. **d.** Spectrophotometric measure of Pgp ATPase, detected in triplicates in NS. *$p<0.05$: T-treated vs. scrambled-treated (-) cells; ***$p<0.001$: KO1/KO2 or T+KO1/KO2 cells vs. scrambled-treated (-) cells; $^{###}p<0.001$: T+KO1/KO2 cells vs. T-treated cells; $^{§§}p<0.01$: T+KO1/KO2 cells vs. KO1/KO2 cells (Student's t-test). **e.** Intracellular content of temozolomide (TMZ), measured in duplicates after cell radiolabelling. ***$p<0.001$: all experimental conditions vs. untreated (-) NS (Student's t-test). **f.** LDH release, measured spectrophotometrically in duplicates. ***$p<0.001$: all experimental conditions vs. untreated (-) AC/NS; $^{###}p<0.001$: T+**1**-treated,

T+KO1/KO2 cells vs. T-treated cells; §§§p<0.001: T+KO1/KO2 cells vs. KO1/KO2 cells (Student's t-test). **g.** Patient #2 NS were lysed and immunoblotted for procaspase and cleaved caspase 3. The figure is representative of one out of three experiments. **h.** Cell viability measured by a chemiluminescence-based assay in quadruplicates. ***p<0.001: all experimental conditions vs. untreated (-) AC/NS; ###p<0.001: T+**1**-treated, T+KO1/KO2 cells vs. T-treated cells; §§§p<0.001: T+KO1/KO2 cells vs. KO1/KO2 cells (Student's t-test).

Figure 5. Compound 1 improves temozolomide efficacy against orthotopically implanted glioblastoma neurosphere-derived tumors

a. Representative *in vivo* bioluminescence imaging of orthotopically implanted patient #2 NS, in animals treated with vehicle (ctrl), compound **1** and temozolomide (TMZ), as follows: 1) control group, treated with 0.2 ml saline solution intravenously (i.v.); 2) **1** group, treated with 3800 ng/kg compound **1** i.v.; 3) TMZ group, treated with 50 mg/kg TMZ *per os* (p.o.); 4) TMZ+**1** group, treated with 50 mg/kg TMZ p.o.+3800 ng/kg compound **1** i.v. (6 animals/group). **b.** Quantification of patient #1-3 NS-derived bioluminescence, taken as index of tumor growth. Data are presented as means±SD (6 animals/group). At day 24: **p<0.005, ***p<0.001: TMZ+**1** group vs. all the other groups of treatment;°°p<0.005, °°°p<0.01: TMZ+**1** group vs. TMZ-group (Student's t-test). **c.** Overall survival probability was calculated using the Kaplan-Meier method. Patient #1 NS: p<0.02: TMZ+**1**-group vs. all the other groups of treatment. Patient #2 NS: p<0.002: TMZ+**1**-group vs. all the other groups of treatment. Patient #3 NS: p<0.001: TMZ+**1**-group vs. ctrl and **1**-group; p<0.05: TMZ+**1** group vs. TMZ-group; p<0.01: TMZ-group vs. ctrl and **1**-group (log rank test; not reported in the figure). **d.** Representative intratumor staining with hematoxylin and eosin (HE) or the indicated antibodies, from patient #2 NS-derived tumors. The photographs are representative of sections from 5 tumors/group of treatment. Bar=10 μm (10× ocular lens, 20× objective). **e.** Quantification of immuno-histochemical images, performed on sections with 111-94

nuclei/field. The percentage of proliferating cells was determined by the ratio Ki67-positive nuclei/total number (hematoxylin-positive) of nuclei using ImageJ software. The ctrl group percentage was considered 100%. The percentage of CAXII, Pgp and caspase 3-positive cells was determined by Photoshop program. Data are presented as means±SD. ***p<0.001: TMZ+**1** group vs. all the other groups of treatment; °°°p<0.001 TMZ+**1** group vs. TMZ-group; ##p<0.005: TMZ vs. ctrl group (Student's t-test). **f**. Immunoblot analysis of the indicated proteins from tumor extracts of patient #2 NS (3 animals/group of treatment).

Figure 1

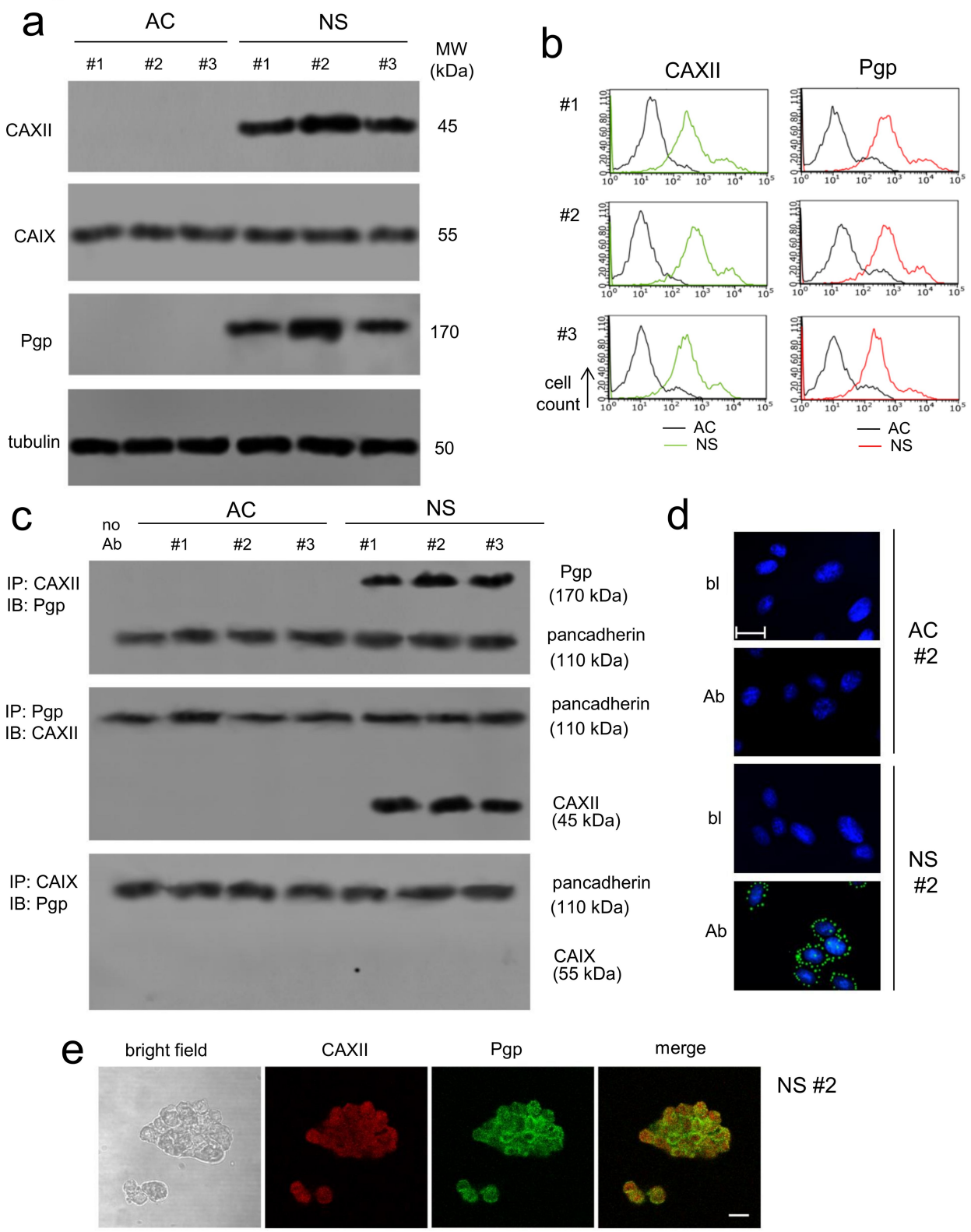
a
AC
NS
#1
#2
#3
#1
#2
#3
MW (kDa)
CAXII
45
CAIX
55
Pgp
170
tubulin
50
b
CAXII
Pgp
#1
#2
#3
cell count
AC
NS
AC
NS
c
no Ab
AC
NS
#1
#2
#3
#1
#2
#3
IP: CAXII
IB: Pgp
Pgp (170 kDa)
pancadherin (110 kDa)
IP: Pgp
IB: CAXII
pancadherin (110 kDa)
CAXII (45 kDa)
IP: CAIX
IB: Pgp
pancadherin (110 kDa)
CAIX (55 kDa)
d
bl
Ab
AC #2
bl
Ab
NS #2
e
bright field
CAXII
Pgp
merge
NS #2

Figure 2

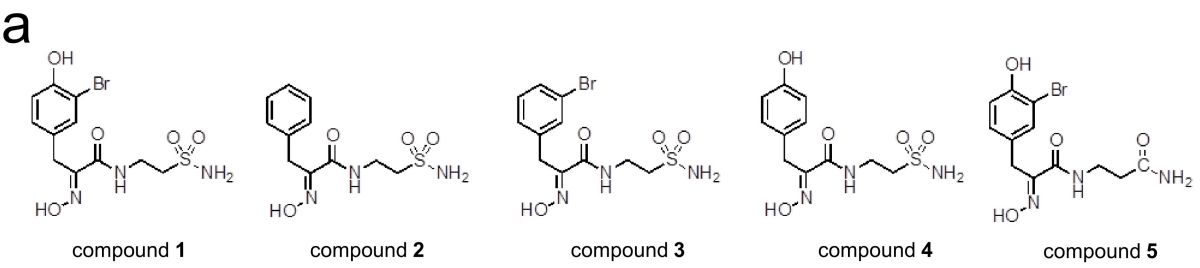
a
compound 1
compound 2
compound 3
compound 4
compound 5
b
Pgp ATPase activity (nmol Pi/min/mg prot)
c
AC
NS
Intracellular doxorubicin (nmol/mg prot)
d
- dox
+ dox
LDH release (% vs total LDH)
AC
NS
e
Viable cells (% vs untreated cells)
AC
NS

Figure 3

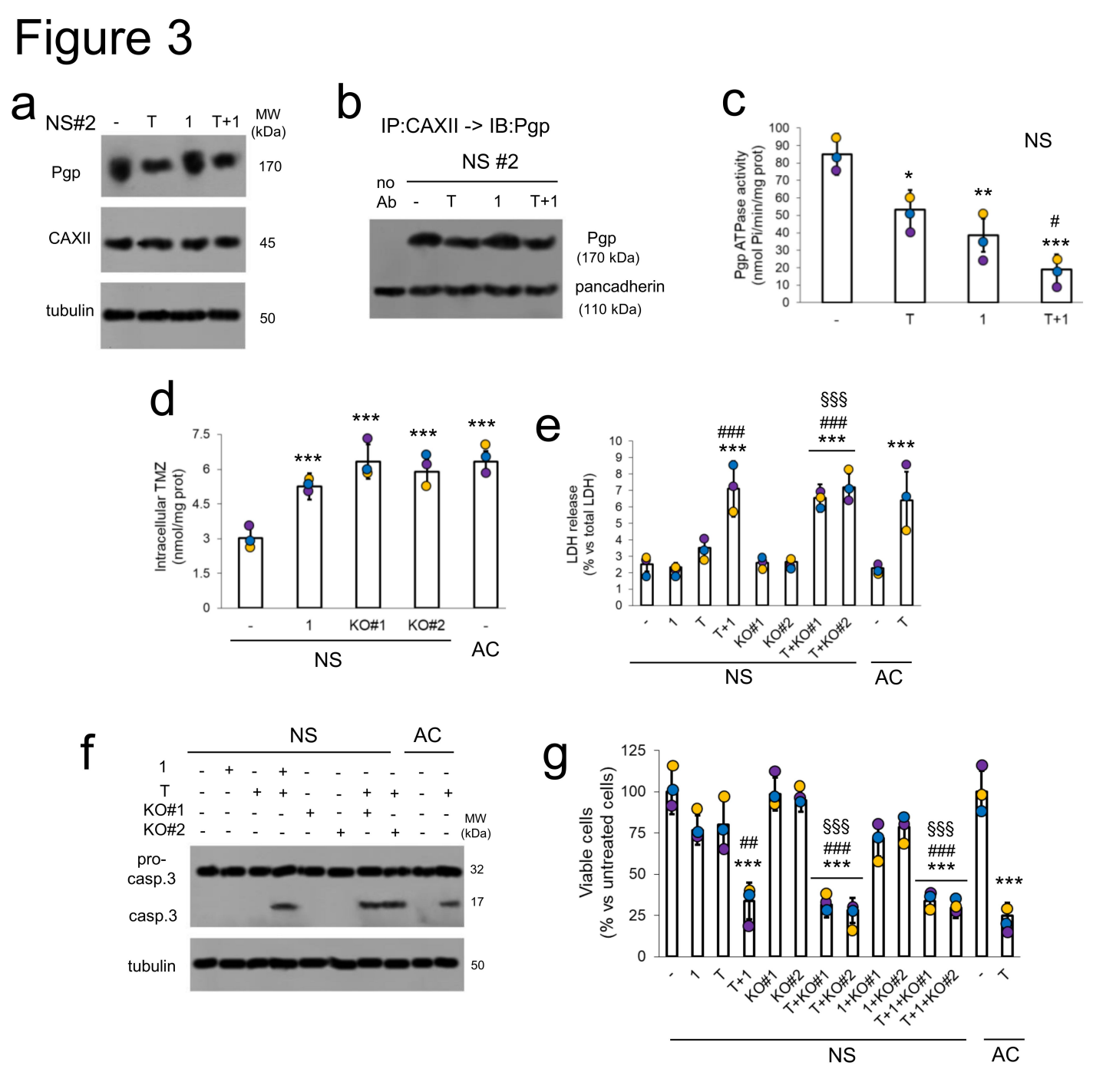
a
NS#2 - T 1 T+1 MW (kDa)
Pgp
170
CAXII
45
tubulin
50
b
IP:CAXII -> IB:Pgp
NS #2
no Ab - T 1 T+1
Pgp (170 kDa)
pancadherin (110 kDa)
c
Pgp ATPase activity (nmol Pi/min/mg prot)
NS
- T 1 T+1
d
Intracellular TMZ (nmol/mg prot)
- 1 KO#1 KO#2 -
NS
AC
e
LDH release (% vs total LDH)
- 1 T T+1 KO#1 KO#2 T+KO#1 T+KO#2 - T
NS
AC
f
NS
AC
1
T
KO#1
KO#2
MW (kDa)
pro-casp.3
casp.3
32
17
tubulin
50
g
Viable cells (% vs untreated cells)
- 1 T T+1 KO#1 KO#2 T+KO#1 T+KO#2 1+KO#1 1+KO#2 T+1+KO#1 T+1+KO#2 - T
NS
AC

Figure 4

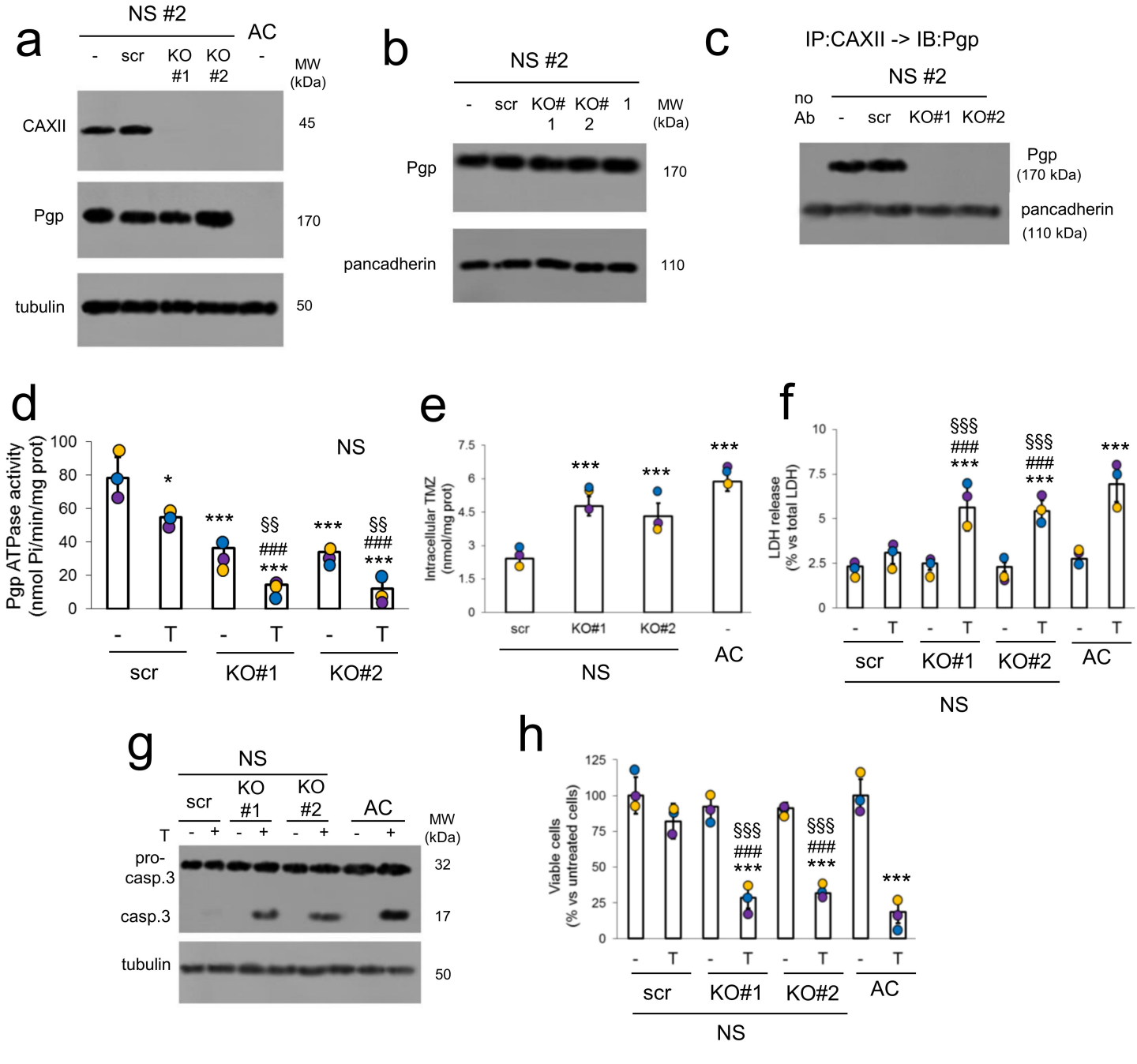
a
NS #2
AC
- scr KO #1 KO #2 -
MW (kDa)
CAXII
45
Pgp
170
tubulin
50
b
NS #2
- scr KO# 1 KO# 2 1
MW (kDa)
Pgp
170
pancadherin
110
c
IP:CAXII -> IB:Pgp
NS #2
no Ab - scr KO#1 KO#2
Pgp (170 kDa)
pancadherin (110 kDa)
d
Pgp ATPase activity (nmol Pi/min/mg prot)
NS
- T - T - T
scr KO#1 KO#2
e
Intracellular TMZ (nmol/mg prot)
scr KO#1 KO#2 -
NS AC
f
LDH release (% vs total LDH)
- T - T - T - T
scr KO#1 KO#2 AC
NS
g
NS
scr KO #1 KO #2 AC
T - + - + - + - +
MW (kDa)
pro-casp.3
32
casp.3
17
tubulin
50
h
Viable cells (% vs untreated cells)
- T - T - T - T
scr KO#1 KO#2 AC
NS

Figure 5

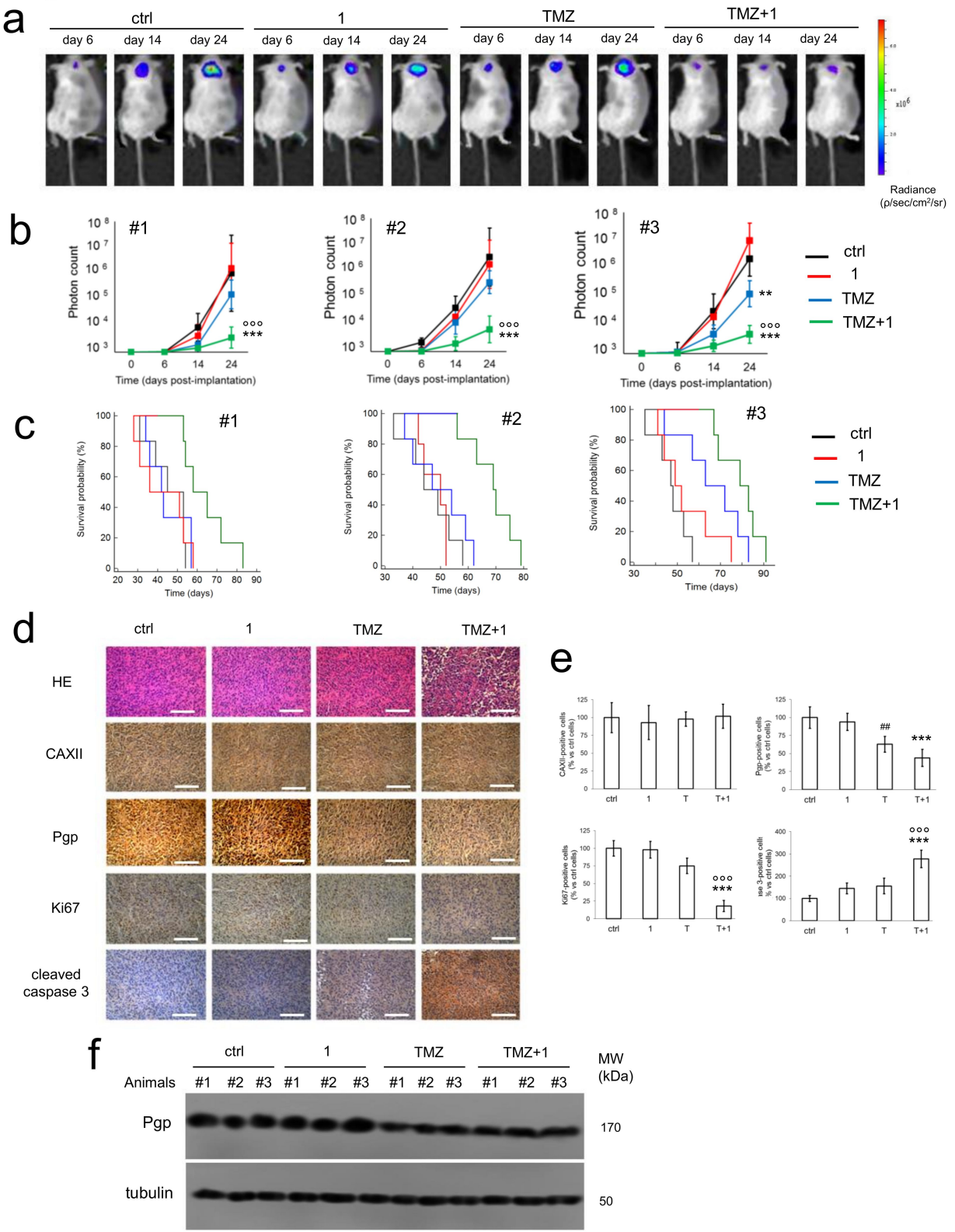
a
ctrl
1
TMZ
TMZ+1
day 6
day 14
day 24
Radiance (p/sec/cm²/sr)
b
#1
#2
#3
Photon count
Time (days post-implantation)
ctrl
1
TMZ
TMZ+1
**
***
°°°
c
Survival probability (%)
Time (days)
d
HE
CAXII
Pgp
Ki67
cleaved caspase 3
e
CAXII-positive cells (% vs ctrl cells)
Pgp-positive cells (% vs ctrl cells)
Ki67-positive cells (% vs ctrl cells)
ase 3-positive cells (% vs ctrl cells)
##
f
Animals
MW (kDa)
Pgp
tubulin
170
50